ELECTROMIGRATION OF Al-Si ALLOY FILMS

James R. Black
Motorola Semiconductor Products Group
5005 E. McDowell Road
Phoenix, Arizona 85008
(602) 244-6201

Abstract

The electromigration characteristics of Al/Si alloys are presented. Below about 210°C the failure mode is an open circuit generated by grain boundary electromigration of Al in Al with an activation energy of 0.54 eV. At higher temperatures the failure mechanism transfers to the electromigration of Si in Al through dislocations with an activation energy of 0.89 eV. The failure is either a shunted junction at (-) ohmic contacts to the metal or an increase in resistance at (+) ohmic contacts.

Introduction

Semiconductor manufacturers often employ aluminum metallization containing 1-3% silicon as an alloying element to manufacture shallow junction devices which require high temperature heat treatments after metallization. This is to prevent shunting underlying or adjacent junctions at ohmic contacts with etch pits filled with Al. These pits can form in the Si substrate at elevated temperatures due to the solid state dissolution and rapid diffusion of Si in thin films of aluminum.[1] The addition of Si as an alloying element to aluminum provides a source to satisfy the solid solubility of Si in Al reducing the dissolution of Si at the ohmic contacts.

van Gurp[2] and Learn[3] have studied the electromigration properties of Al/Si alloy films. The former studied non-glassed, very small grained Al/Si films of 0.3% and 1.8% Si as well as pure Al. When stressed at a current density of 2×10^6 A/cm^2 the pure Al exhibited an activation energy of 0.55 eV with voiding randomly distributed down the stripe. The 0.3% Si alloy had an activation energy of 0.32 eV while the 1.8% alloy had an activation energy of 0.31 eV. At 200°C the 0.3% Si alloy had a lifetime five times greater than pure Al while the 1.8% alloy exhibited an order of magnitude improvement over pure aluminum. The failure mechanism for the alloys was a void which always formed at the negative end of the stripe indicating excessive gradients in temperature or current density at that region. The low activation energy was attributed to surface diffusion.

Learn's [3] results on non-glassed silicon alloy of aluminum were similar exhibiting longer lifetime at elevated temperatures than pure Al, but because of the lower activation energy the pure Al films provided greater lifetime below about 120°C. Neither investigator reported on the electromigration of Si through Al.

In addition to electromigration device failure by void formation in the conductor, it has been known that other device failure modes could be generated by the electromigration of Si through Al.[4,5,6] This present study was initiated to better understand the electromigration characteristics of the Al/Si alloy system.

Solid State Solubility of Si In Al

Since only those Si ions which are dissolved in Al are capable of electromigrating through the alloy, it is important to understand the solubility of Si in Al as a function of temperature.

Aluminum and silicon form a simple eutectic system. A portion of the phase diagram is shown in Figure 1.[7] The pie shaped region labeled (Al) is a solid region whose crystalline structure is identical to pure aluminum except that some of the aluminum ions have been substituted by silicon ions. This is the region of "solid solution." The lower curved boundary of that region is called the "solvus" curve and defines the maximum amount of silicon that can dissolve into aluminum as a function of temperature.

Below and to the right of the solvus curve is a solid region containing a mixture of essentially pure silicon crystals and crystals whose composition is determined by the solvus curve. As shown, below about 200°C well annealed aluminum silicon alloys consist of a mixture of nearly pure aluminum and pure silicon crystals. When aluminum in contact with silicon is heated silicon rapidly dissolves by a solid state diffusion process (below 577°C) into the aluminum to saturate the solution at a composition determined by the solvus curve. Upon cooling the dissolved silicon precipitates out of solution forming a mixture of silicon and aluminum crystals.

Diffusion of Si In Al Films

The diffusivity of Si in thin film Al is much higher than in bulk samples. McCaldin and Sankur[1] as well as Nanada[8] observed the diffusion to be about 50 times greater in the films than in bulk material at 400°C and diffusion activation energies of 0.79 eV and 1.05 eV respectively (Figure 2). van Gurp studied the diffusion of Si in Al films at lower temperatures and reported an activation energy of 0.9 eV.[9] These activation energies are appreciably lower than the bulk (θ = 1.33 eV)[10] and is attributed to a much stronger grain boundary and dislocation contribution. For example, at 500°C a silicon atom moves nearly 1 1/2 microns a second in thin aluminum films!

Low Temperature Al/Si Alloy Electromigration

Because it was recognized that two basic processes could take place when Al/Si alloys are subjected to stress which results in electromigration, two experiments were designed to study these.[4] One electromigration process which takes place below about 230°C is the electromigration of aluminum ions through the aluminum matrix resulting in the growth of voids that eventually cause failure due to an open electrical circuit. The second process is the electromigration of silicon through the aluminum matrix which could cause device failure by the growth of pits in silicon at negative contacts to the aluminum or could cause an increase in resistance at positive silicon contacts due to the build up of resistive silicon at those contacts. This failure mechanism occurs at elevated temperatures above about 230°C. This section describes experiments designed to study the electromigration of Al in Al while the following section addresses the electromigration of Si in Al.

Three different alloys were selected with silicon contents being 0.79%, 1.9% and 3% Si. These were deposited by co-evaporation from two electron beam heated sources onto 900 Å thick SiO_2 on Si single crystal substrates. The grain size was about 1.4 microns and the silicon had segregated as particles attached to the SiO_2 with a particle density ranging from 3.75×10^8 to

Authorized licensed use limited to: PORTLAND STATE UNIVERSITY. Downloaded on March 29, 2009 at 03:40 from IEEE Xplore. Restrictions apply.

5.7×10^8 per cm^2. The 0.70 to 0.73 micron thick films were etched into fine line conductors with a nominal width of 4×10^{-4} inches and a length of 3×10^{-2} inches. One half of the films received a silicon etch treatment to remove the residual silicon particles located on the field oxide after the aluminum etch. The films were coated with an 8000 Å thick layer of chemical vapor deposited glass containing 3% phosphorus. The individual die were bonded to TO-3 headers and wire bonded with 5×10^{-3} inch diameter aluminum wire. Finally caps were welded to the parts under a nitrogen ambient.

The data obtained during this experiment are summarized in Table I. The letter following the run number indicates the alloy used where A = 0.79% Si, B = 1.9% Si and C = 3% Si. The current density ranged from 6.6×10^5 to 2×10^6 A/cm^2 while the temperature varied from 110°C to 210°C. The film cross sectional areas and the metal grain sizes were relatively invariant. The median time to failure for these thirty experiments varied from 68 hours to 630 hours and the standard deviations ranged from 0.23 to 0.65 with the majority grouped near the average of 0.40.

Groups of identical parts containing between 15 and 20 devices each were subjected to the same current density and temperature stress. Generally the test continued until all or nearly all devices failed. An electronic recorder was utilized to record the time required for each device to fail. The data followed a log-normal distribution as shown in Figure 3 which shows the cumulative percent of the failed devices in one of the test runs plotted vs. time in hours on log-normal probability paper. The median time to failure and the standard deviation, σ, for each run was determined from such plots.

All film failures were due to voids growing in the film which eventually formed electrically open circuits. The voids were randomly distributed along the stripes with many of them of sufficient size to nearly create an open circuit. Figure 4 presents SEM micrographs of voids which were typical of those distributed down the length of the stripes. Cracked passivation glass was also observed distributed along the length of the stripes which was caused by the accumulation of metal ions exerting sufficient pressure on the glass to fracture it. One of these regions before and after removal of the passivation glass is presented in Figure 5. No difference was observed in the electromigration behavior between those films which received an etch to remove the residual silicon in areas cleared of aluminum and those which contained the residual silicon.

Arrhenius plots of the results for each alloy gave close fits to a straight line with activation energies between 0.54 and 0.55 eV. These were nearly coincidental with a slight tendency for greater lifetime as the silicon content increased. This effect was small and is believed to be within experimental error.

A combined Arrhenius plot of the three alloys including all thirty data points is presented in Figure 6. In this figure the ordinant is the log of the film cross sectional area divided by the current density squared and the median time to failure. The least squares method was used to determine the 50% failure line. Following Peck[11] the percentile lines were calculated using the average sigma of the thirty test cells and the log-normal distribution. The equations derived from this plot which describe the median lifetime are:

$$\frac{wt}{J^2\ MTF} = 4.727 \times 10^{-16} \exp - \frac{0.544}{kT}$$

$$\text{and } MTF = \frac{wt}{J^2}\ 2.116 \times 10^{15} \exp \frac{0.544}{kT}$$

where K is Boltzmann's constant 8.62×10^{-5} eV/°K

T is the absolute temperature of the film

W is the film width in cm

and t is the film thickness in cm.

The activation energy of 0.544 eV is a value generally accepted for the self diffusion of Al down grain boundaries.

It is of interest to note that the lifetime of the passivated alloy films are 2-3 times greater than pure small grained aluminum that was not passivated. (Compare Figure 4 with Figure 2 in Reference 5.) This can be attributed to the passivation glass which restricts hillock growth causing the metal to go under compression. This compressive stress in turn applies a force to the electromigrating ion which is opposite to that due to the electron wind force resulting in increased lifetime.[12] Satake et. al.[13] reported that a 5000 Å thick SiO_2 passivation glass increased electromigration lifetime of small grained Al films a factor of two over non-glassed films. In view of this it is concluded that the silicon addition to aluminum has very little effect on its rate of electromigration. At temperatures below about 210°C failure is due to the grain boundary electromigration of aluminum in aluminum forming voids and producing an electrical open circuit.

High Temperature Al/Si Alloy Electromigration

When silicon electromigrates at elevated temperatures in Al/Si alloy films the definition of device failure must be redefined since the failure is not an open circuit. It could be defined as a shorted junction at a silicon-aluminum contact where electrons leave the silicon and enter the aluminum. Alternately it could be defined as a given rise in contact resistance at aluminum-silicon contacts where electrons leave the aluminum and enter the silicon.

To study this high temperature mode of Al/Si alloy electromigration failure a test vehicle was constructed where the contacts to the Al/Si alloy stripes were made to silicon at each end of the stripes. Figure 7 is a cross sectional diagram of the structure which consists of an n type substrate with boron diffused contact regions 1.35 µm deep. The parts were passivated in a manner identical to that in the previous experiment. The separated die were then bonded to TO-3 headers, wire bonded with 5 mil diameter aluminum wires using those stripes with nominal 0.4 x 0.4 mil ohmic contacts. The parts were then capped in a nitrogen ambient.

The silicon alloys used for this experiment were 0.35% Si, 1.4% Si, 2.5% Si and 3.6% Si. Half of the devices contained residual silicon in the areas cleared of aluminum during metal patterning while half of the devices had this residual silicon removed. The cross sectional areas of the alloy films varied from 8.669×10^{-8} cm^2 to 10.234×10^{-8} cm^2. The devices were placed under electromigration stress conditions at temperatures ranging between 240°C and 311°C with monitors for open circuits, resistance build up and negative terminal shorting. For this test device, it was not known at the start of the experiment which failure mode would predominate.

The failures exhibited a bimodal distribution when plotted on log-normal probability paper as shown in Figure 8. When this set of devices was inspected utilizing an optical microscope it was determined that six of the devices failed by the formation of voids randomly distributed along the stripes with one void per stripe eventually forming an open circuit. Five of the devices in this set failed due to etch pits which formed in the silicon at the negative terminals eventually shorting

Authorized licensed use limited to: PORTLAND STATE UNIVERSITY. Downloaded on March 29, 2009 at 03:40 from IEEE Xplore. Restrictions apply.

the junction. It was determined that the flat portion of the curve represented failure by void formation while the steep portion were those devices which failed by junction shorting. To study these failure modes each group within a set which failed either by the electromigration of aluminum in aluminum or by the electromigration of silicon in aluminum was treated as a separate set from which the median time to failure and the standard deviation were determined from log-normal plots. Unfortunately the sample sizes were not as great as desired introducing some scatter in the data.

Figure 9 presents SEM micrographs of the positive and negative terminals of a glass passivation stripe that had been stressed at $310^{o}C$ at a current density of 4.95×10^{5} A/cm^2. A pile up of Al and Si is observed at the (+) terminal cracking the glass passivation. Also a depression is observed at the (-) terminal where the Al and Si has been depleted also causing the passivation glass to crack. A hillock is also presented which has cracked the glass and pushed up through it. Figure 10 shows the same features as does Figure 8, however, the passivation glass has been etched away revealing the metal. Metal is observed to accumulate at the (+) terminal while pitting of the Si substrate has occurred at the (-) terminal. The Al/Si alloy is also shown to have formed a void near the (-) terminal. The hillock appears flattened and distorted compared to the free growing structures found on non-glassed films.

Figure 11 shows the same terminals as were presented in Figures 9 and 10, however, the aluminum metal has been selectively etched away. It is observed that the alloy build up at the positive terminal consisted of silicon being deposited at the silicon contact with aluminum on top of it. Coarsening of the silicon particles has occurred around the ohmic contact but appear depleted at the higher current density regions. The negative terminal exhibits severe vertical and lateral pitting with silicon build up near the contact where the current density drops due to radial spreading. Silicon build up is not observed where the alloy formed a void at the contact and therefore was not connected to the silicon source. In the stripe the silicon was observed to coarsen in an elongated fashion decorating aluminum grain boundaries.

Typical void formation and hillock growth due to the electromigration of aluminum are shown in Figure 12. The passivation glass has been etched off of three of the four stripes shown.

Table II presents the high temperature test conditions and results obtained. Four alloys were used ranging from 0.35% to 3.6% Si. The temperature ranged from $240^{o}C$ to $311^{o}C$ and the current density varied from 4.565×10^{5} A/cm^2 to 1.038×10^{6} A/cm^2. In general at the lower temperatures the predominant failure mode was due to the electromigration of Al in Al while at the higher temperatures the failure mode gradually switched to that due to the electromigration of Si in Al. No effect was observed that was a function of the Si content of the alloys.

An Arrhenius plot of the data for failures due to the electromigration of Si in Al is presented in Figure 13. This relates the Al/Si alloy median time to failure due to this failure mode to the film geometry current density and temperature. The line drawn through the experimental points constructed using the least squares technique can be expressed as:

$$\frac{wt}{J^2 \, MTF} = 2.275 \times 10^{-13} \exp(-0.889/kT)$$

from which: $$MTF = \frac{wt}{J^2} 4.396 \times 10^{12} \exp(0.889/kT)$$

The activation energy of 0.89 eV agrees well with the work of van Gurp[9] who studied the thin film precipitation of Si from a supersaturated Al/Si solid solution by resistance measurements and by microscopy. He found the activation energy for the diffusion of Si in Al for Al - 1.8 at % Si and Al - 0.8 at % Si to be 0.9 ± 0.05 eV (See Fig. 2).

The equations given above relate only to the specific test device used which failed by a shorted (-) contact junction whose contact area was about 83 μm^2, the junction depth was 1.35 μm and the conductor cross sectional area was about 9.2×10^{-8} cm^2. Devices which are more sensitive to silicon electromigration (smaller contact areas, shallower junctions, larger conductor cross sectional areas to contact area ratios, more sensitive to increased resistance at the positive contacts) would be expected to operate along lines parallel to that of Figure 13 but moved upward. The preexponential constant for the first equation given would increase while that of the second equation would decrease.

In a like manner devices which are less sensitive to the effects of the electromigration of Si through Al would be expected to possess plots with slopes similar to that of Figure 13 but below that of Figure 13.

Figure 14 presents an Arrhenius plot of the data taken where the failure was an open circuit caused by the electromigration of Al in Al. Due to the generally small sample sizes available and the fact that some of the electrical opens appeared around the (-) terminal contact the data points were somewhat scattered. Using the least squares technique a line drawn through these points exhibited an activation energy of 0.7 eV. Rather than use that line the median time to failure line obtained at lower temperatures where failures were due to electrical opens caused by the electromigration of Al in Al (See Figure 6) was extrapolated to higher temperatures and is included in Figure 14. This indicates that at high temperatures the electromigration of Al through Al behaves similarly to that at low temperatures.

A composite Arrhenius plot of glassed Al/Si small grain alloy median time to failure as a function of film geometry, current density and temperature where failures occur due to the electromigration of Al in Al or Si in Al for the test device used is presented in Figure 15. Except at the very high temperatures ($T > 210^{o}C$) devices constructed with Al/Si alloy metallization would be expected to fail by an open circuit due to the electromigration of Al in Al. Those devices which are very sensitive to the effects of electromigration of Si in Al may have to be limited to a lower maximum junction temperature.

Conclusion

Under normal device operation at temperatures below about $210^{o}C$ the electromigration characteristics of small grain aluminum-silicon alloy films are nearly identical to pure small grain aluminum films. The failure is an open circuit due to the growth of voids in the aluminum alloy resulting from the electromigration of Al ions in an Al crystal matrix. The activation energy for the process of 0.54 eV indicates that the electromigration takes place mainly down Al grain boundaries.

At elevated temperatures the electromigration failure mechanism is due to the electromigration of Si through Al. The activation energy of 0.89 eV is attributed to the electromigration of Si through dislocations and grain boundaries in Al. Two failure modes

Authorized licensed use limited to: PORTLAND STATE UNIVERSITY. Downloaded on March 29, 2009 at 03:40 from IEEE Xplore. Restrictions apply.

may result due to this process. One is the growth of etch pits at (-) terminals caused by the depletion by electromigration of dissolved silicon in the aluminum contacting the silicon. This enables further dissolution of the underlying silicon into the aluminum. This process is a continuous one resulting in a shunted underlying or adjacent junction where a pit filled with Al penetrates the junction. Different devices will be more or less sensitive to this failure mode depending upon the junction depth, the lateral distance between the metal and the adjacent junction, the size of the contact, current density, temperature, etc. Radio frequency power transistors often fail by this mechanism when life test stressed at elevated temperatures.[14] This type of failure can also occur with pure Al metallization.

A second failure mode brought about by the electromigration of Si through Al is due to an increase in resistance at an ohmic contact where the electrons leave the alloy and enter Si. At these contacts the electromigrating Si precipitates out of the saturated solution and grows on the Si crystal substrate.[15] The deposited Si is resistive and can cause device failure with various devices having their own sensitivity to failure by this process. This failure mode generally occurs at elevated temperatures during device life tests.

Acknowledgment

This work was sponsored by the Air Force Systems Command, Rome Air Development Center, Griffiss Air Force Base, New York 13441 under Contract No. F 30602-76-C-0300.

References

1. J. O. McCaldin and H. Sankur, "Diffusivity and Solubility in the Al Metallization of Integrated Circuits," Appl. Phys. Lett. 19, (1971) 524.

2. G. J. van Gurp, "Electromigration in Aluminum Films Containing Si," Applied Physics Letters, Vol. 19, No. 11 (1971) 476.

3. A. J. Learn, "Electromigration Effects in Aluminum Alloy Metallization," J. Electronic Materials, 3, No. 2 (1974) 531.

4. J. R. Black, "Metallization Failures in Integrated Circuits," Tech. Report No. RADC-TR-68-243 Rome Air Development Center, Air Force Systems Command, Griffiss Air Force Base, New York, October 1968.

5. J. R. Black, "Electromigration Failure Modes in Aluminum Metallization for Semiconductor Devices," Proc. IEEE, Vol. 57, No. 9, Sept. 1969.

6. J. R. Black, "Etch Pit Formation in Silicon at Aluminum-Silicon Contacts Because of Transport of Silicon in Aluminum by Momentum Exchange with Conducting Electrons," Ohmic Contacts to Semiconductors, B. Schwartz Ed., The Electrochemical Society, Inc., N.Y. 1969.

7. M. Hansen, Constitution of Binary Alloys," 2nd Edition, McGraw-Hill, New York, 1958.

8. M. Nanda, "Diffusion of Impurities in Thin Aluminum Films," Extended Abstracts Electrochemical Society Meeting, Atlantic City (1970) 478.

9. G. J. van Gurp, "Diffusion-Limited Si Precipitation in Evaporated Al/Si Films," J. Appl. Physics, 44, No. 5 (1973).

10. C. J. Smithells, "Metals Reference Book," Vol 2, 4th Ed., Plenum Press, New York, 662.

11. D. S. Peck, "The Analysis of Data from Accelerated Stress Tests," 9th Annual Proceedings, Reliability Physics, IEEE Catalog No. 71-C-9-Phy., 1971, p 69.

12. I. A. Blech, "Electromigration in Thin Films on Titanium Nitride," J. Appl. Phys. Vol. 47, No. 4, April 1976.

13. T. Satake, K. Yokoyama, S. Shirakawa and K. Sawaguchi, "Electromigration in Aluminum Film Stripes Coated with Anodic Aluminum Oxide Films," Jap. J. Appl. Physics, Vol. 12, No. 4, April 1973.

14. S. Gattesfeld, "A Life Test Stdy of Electromigration in Microwave Power Transistors," 12th Annual Proceedings Reliability Physics 1974, IEEE Cat. No. 74CH0839-1 Phy., 1974 p 94.

15. E. T. Lewis, D. Bartels, A. A. Capobianco, "Reliability Evaluation of ECL Microcircuits," RADC-TR-193, Rome Air Development Center, Air Force Systems Command, Griffiss Air Force Base, New York, 13441, June 1976.

Authorized licensed use limited to: PORTLAND STATE UNIVERSITY. Downloaded on March 29, 2009 at 03:40 from IEEE Xplore. Restrictions apply.

TABLE I

Low Temperature Al/Si Alloy Test Conditions and Results

Run #	Current ma	Film Area cm² x 10⁸	Temperature °C	$\frac{10^3}{K}$	Current Density A/cm² x 10⁻⁶	MTF hours	Std. Dev. σ	$\frac{wt}{J^2 MTF}$ x 10²²
1A	61.07	7.64	167	2.273	0.80	288	.34	4.14
1B	60.18	7.16	167	2.273	0.84	345	.44	2.94
1C	59.55	6.95	167	2.273	0.86	380	.43	2.44
2A	58.14	7.63	190	2.160	0.76	202	.44	6.51
2B	63.01	7.16	190	2.160	0.80	213	.65	5.36
2C	58.11	7.30	190	2.160	0.80	223	.37	5.17
3A	63.18	7.63	210	2.070	0.83	125	.34	8.90
3B	56.95	7.16	210	2.070	0.80	139	.63	8.14
3C	58.12	7.30	210	2.070	0.80	139	.40	8.28
4A	76.90	7.69	167	2.273	1.00	170	.48	4.52
4B	72.48	7.22	167	2.273	1.00	269	.35	2.68
4C	69.75	6.95	167	2.273	1.00	280	.35	2.46
5A	76.38	7.69	192	2.151	0.99	105	.23	7.42
5B	78.20	7.22	192	2.151	1.08	89	.49	6.93
5C	73.20	6.95	192	2.151	1.05	129	.45	4.85
6A	76.98	7.69	210	2.070	1.00	68	.52	11.3
6B	71.34	7.22	210	2.070	0.99	75	.45	9.86
6C	69.14	6.95	210	2.070	1.00	85	.41	8.26
7A	152.2	7.69	110	2.611	2.00	560	.46	0.342
7B	143.4	7.16	110	2.611	2.00	560	.36	0.321
7C	146.2	7.30	110	2.611	2.00	493	.38	0.369
8A	154.	7.69	137	2.44	2.00	178	0.23	1.07
8B	144.	7.22	137	2.44	1.98	245	0.31	0.75
8C	139.	6.95	137	2.44	1.98	292	0.47	0.61
9A	75.66	7.69	154	2.34	0.98	326	0.33	2.44
9B	72.38	7.22	154	2.34	1.00	346	0.46	2.01
9C	69.72	6.95	154	2.34	1.00	630	0.34	1.10
10A	154.	7.69	123	2.52	2.01	300	0.50	0.64
10B	144.	7.22	123	2.52	2.00	339	0.26	0.53
10C	139.	6.95	123	2.52	2.00	382	0.24	0.46

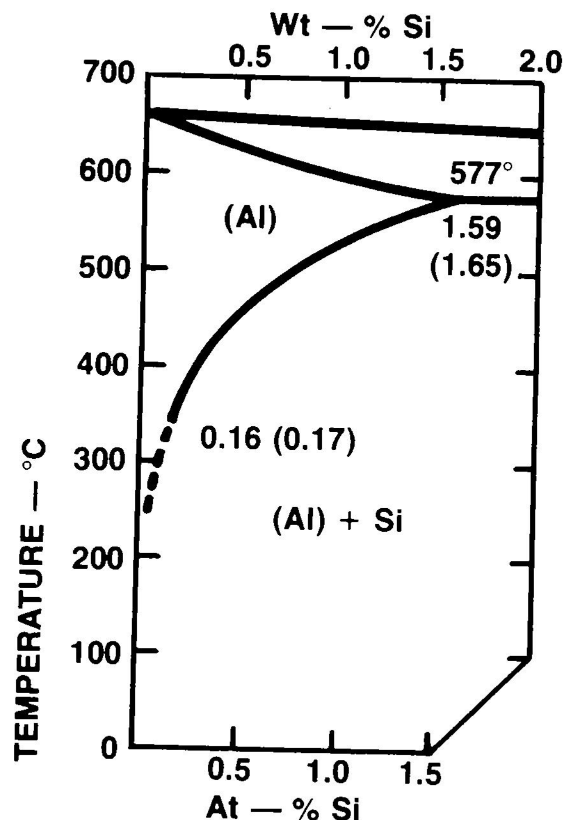

Figure 1. Aluminum-silicon phase diagram.

TABLE II

High Temperature Al/Si Alloy Test Conditions and Results

Run #	Failure Mode	Alloy	Film Area x 10⁸ cm²	Temperature C	$\frac{10^3}{K}$	Current Density A/cm² x 10⁻⁶	MTF hours	Std. Dev. σ	$\frac{wt}{J^2 MTF}$ x 10²²
1	40% Si in Al	3.6% Si	8.771	260	1.876	1.0	61	.14	14.38
1	60% Al in Al	3.6% Si	8.771	260	1.876	1.0	21	.48	41.77
2	62% Si in Al	3.6% Si	8.771	300	1.745	0.498	114	.11	30.96
2	38% Al in Al	3.6% Si	8.771	300	1.745	0.498	65	.12	54.30
3	100% Si in Al	3.6% Si	8.771	310	1.715	0.495	85	.40	42.15
4	50% Si in Al	1.4% Si	8.669	260	1.876	0.8057	202	.36	6.574
4	50% Al in Al	1.4% Si	8.669	260	1.876	0.8057	92	.38	14.43
4	55% Si in Al	2.5% Si	9.150	260	1.876	0.8015	215	.36	6.624
4	45% Al in Al	2.5% Si	9.150	260	1.876	0.8015	60	.73	23.74
4	64% Si in Al	0.35% Si	10.234	260	1.876	0.7944	154	.49	10.53
4	36% Al in Al	0.35% Si	10.234	260	1.876	0.7944	56	.32	28.95
5	80% Si in Al	0.35% Si	10.234	311	1.712	0.4565	84	.26	58.49
5	20% Al in Al	0.35% Si	10.234	311	1.712	0.4565	60	.14	81.89
6	20% Si in Al	1.4% Si	8.669	240	1.949	1.038	245	—	3.543
6	80% Al in Al	1.4% Si	8.669	240	1.949	1.038	93	.48	9.333
6	45% Si in Al	2.5% Si	9.150	240	1.949	1.030	174	.71	4.952
6	55% Al in Al	2.5% Si	9.150	240	1.949	1.030	75	.10	11.49
6	100% Al in Al	3.5% Si	8.771	240	1.949	1.037	49	.76	16.65

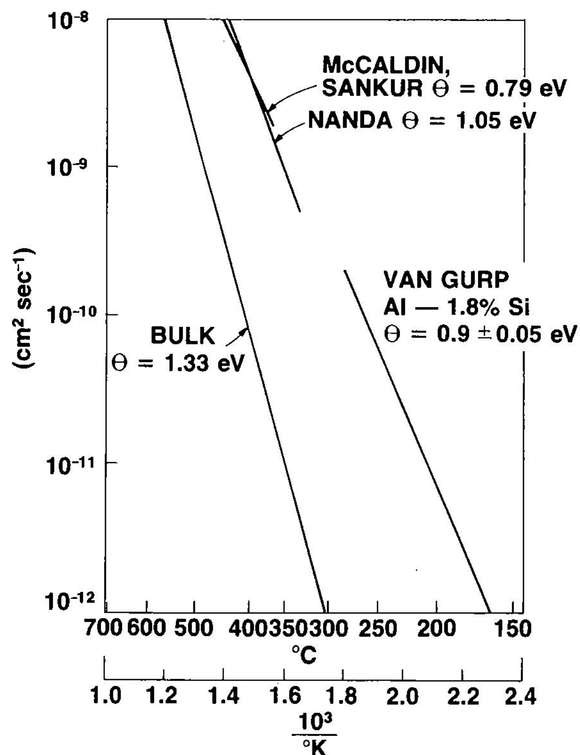

Figure 2. The diffusivity of silicon in solid aluminum.

Authorized licensed use limited to: PORTLAND STATE UNIVERSITY. Downloaded on March 29, 2009 at 03:40 from IEEE Xplore. Restrictions apply.

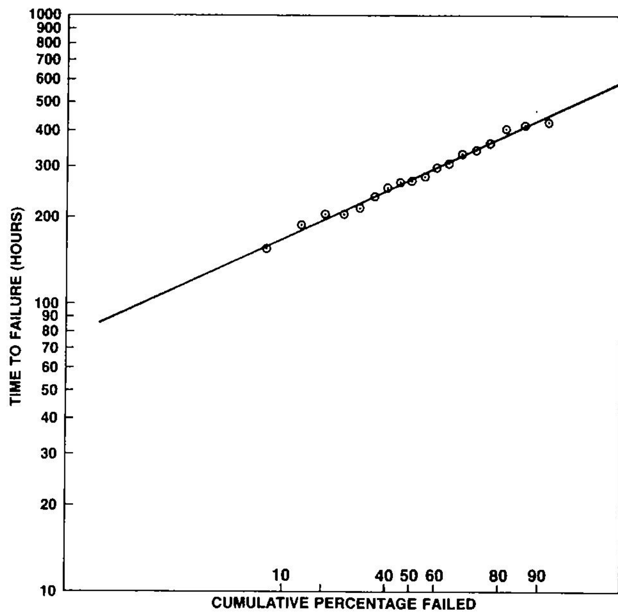

Figure 3. Log normal plot of a 19 device cell stressed at 167°C at $J = 8 \times 10^5$ A/cm^2.

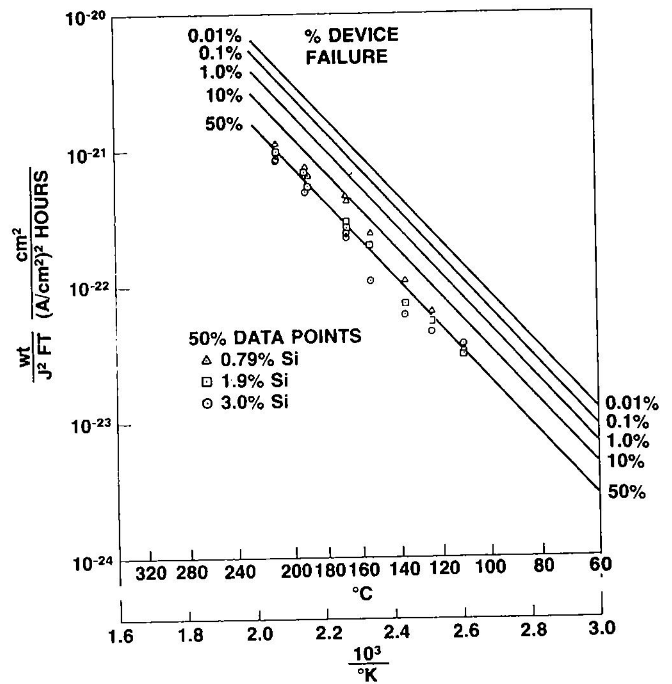

Figure 6. Combined Al/Si alloy data relating % device failure time to film geometry, current density and temperature.

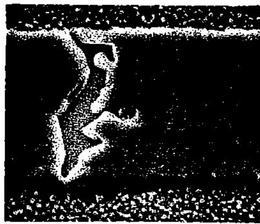

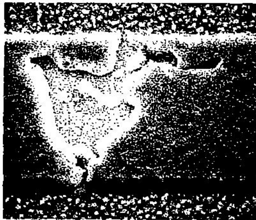

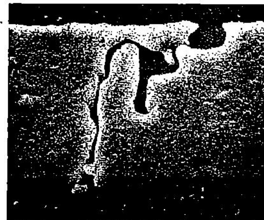

VOIDS FORMED IN Al/Si ALLOYS DURING ELECTROMIGRATION TEST AT LOW TEMPERATURES.

Figure 4.

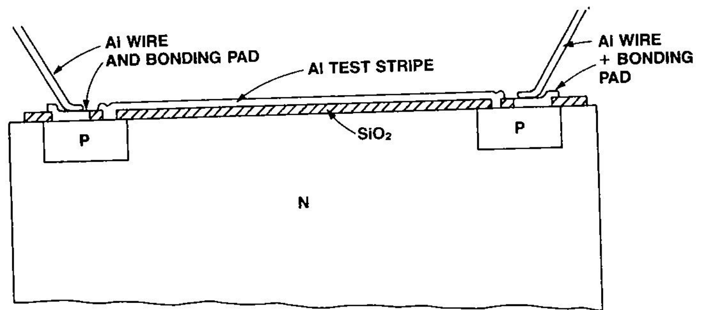

Figure 7. Schematic of high temperature test structure cross section prior to passivation.

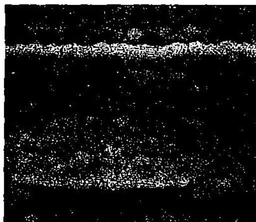

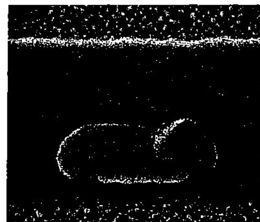

CRACKED PASSIVATION GLASS DUE TO HILLOCK GROWTH BEFORE AND AFTER GLASS REMOVAL.

Figure 5.

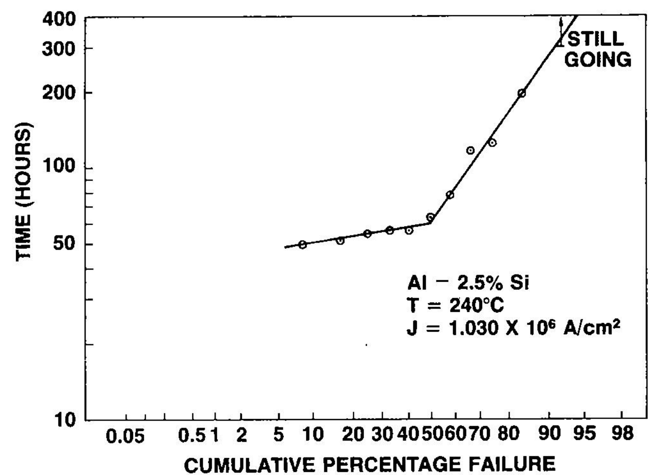

Figure 8. High temperature bimodal failure distribution.

Authorized licensed use limited to: PORTLAND STATE UNIVERSITY. Downloaded on March 29, 2009 at 03:40 from IEEE Xplore. Restrictions apply.

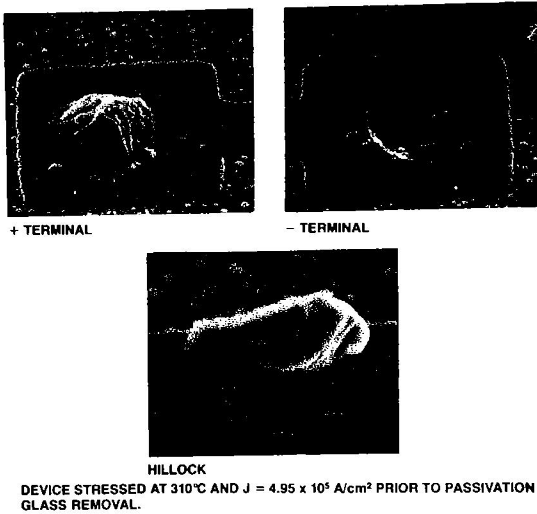

DEVICE STRESSED AT 310°C AND J = 4.95 x 10^5 A/cm² PRIOR TO PASSIVATION GLASS REMOVAL.

Figure 9.

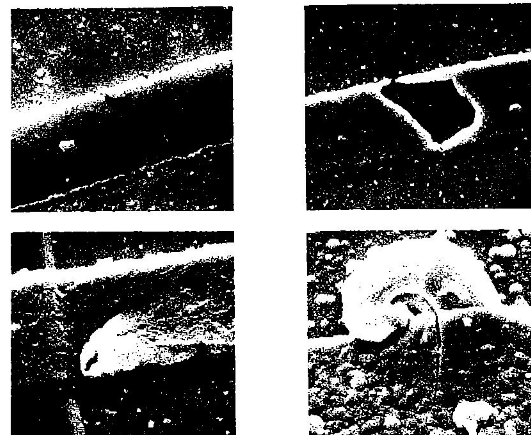

TYPICAL VOIDS AND HILLOCKS OBSERVED IN HIGH TEMPERATURE Al/Si FILMS DUE TO ALUMINUM ELECTROMIGRATION IN Al.

Figure 12.

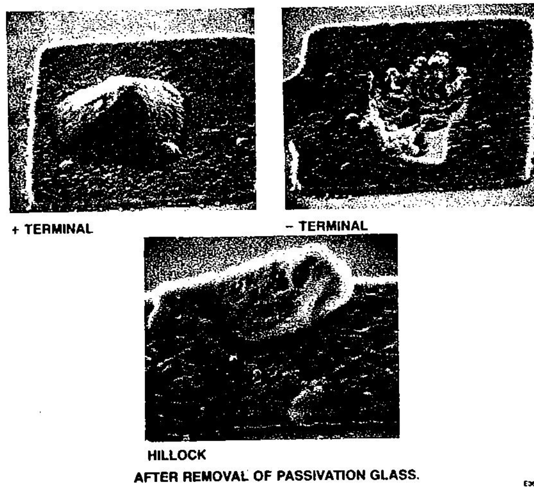

AFTER REMOVAL OF PASSIVATION GLASS.

Figure 10.

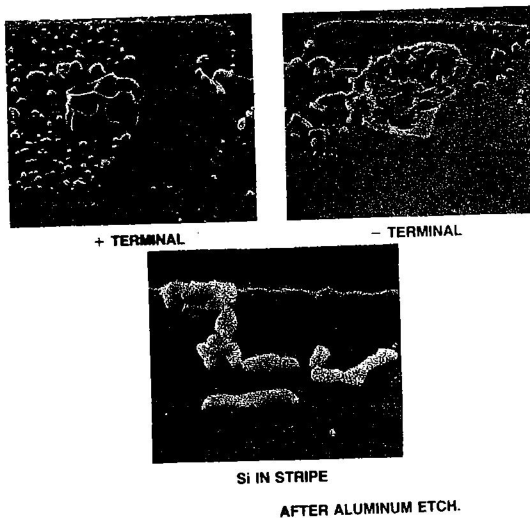

AFTER ALUMINUM ETCH.

Figure 11.

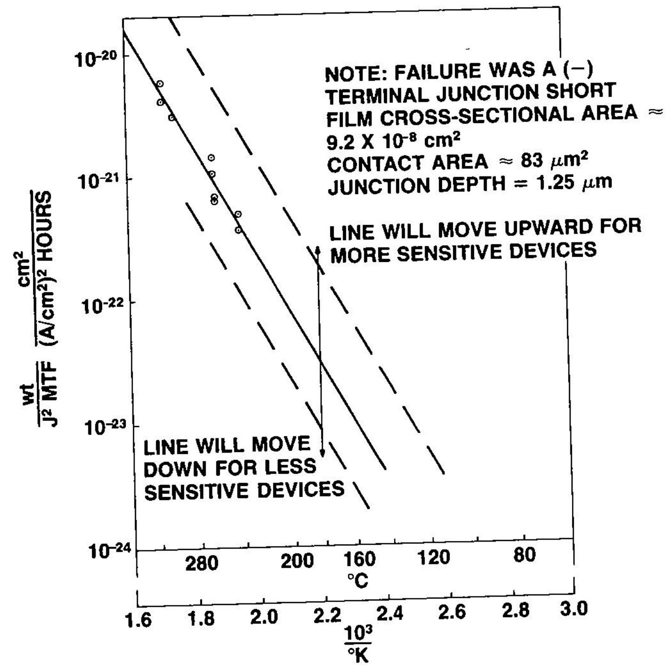

Figure 13. Al/Si alloy median time to failure due to electromigration of Si in Al related to film geometry, current density and temperature.

Authorized licensed use limited to: PORTLAND STATE UNIVERSITY. Downloaded on March 29, 2009 at 03:40 from IEEE Xplore. Restrictions apply.

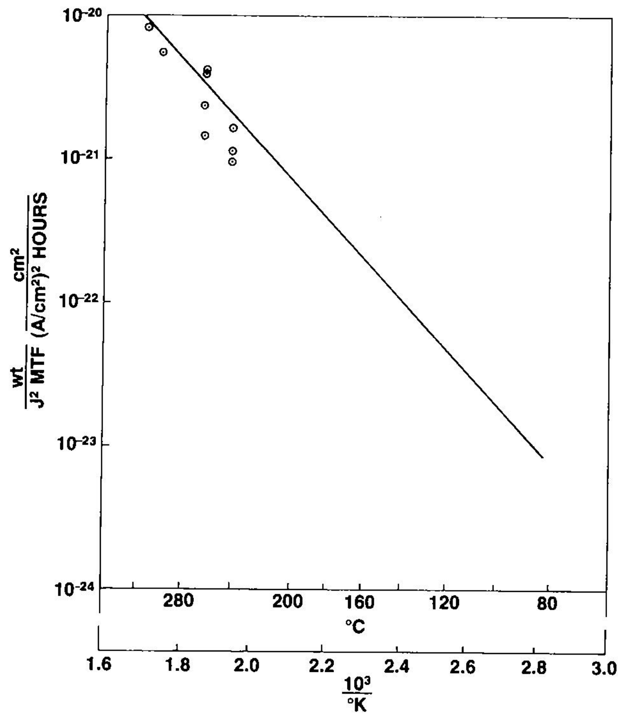

Figure 14. Al/Si alloy median time to failure due to void formation related to film geometry, current density and temperature.

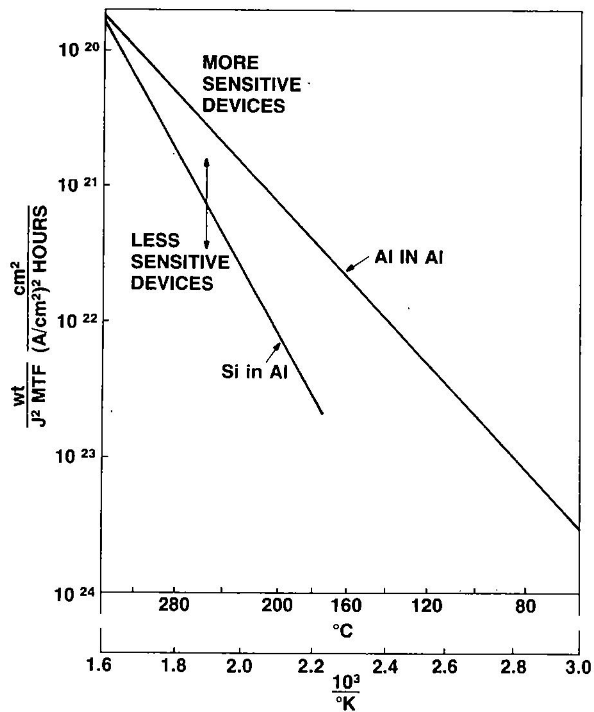

Figure 15. Al/Si alloy failures due to the electromigration of Al in Al and Si in Al.

Authorized licensed use limited to: PORTLAND STATE UNIVERSITY. Downloaded on March 29, 2009 at 03:40 from IEEE Xplore. Restrictions apply.